

## Polarization-dependent beam switch based on an *M*-plane GaN/AlN distributed Bragg reflector

D. M. Schaadt<sup>a)</sup> and O. Brandt<sup>b)</sup>

*Paul-Drude-Institut für Festkörperelektronik, Hausvogteiplatz 5-7, 10117 Berlin, Germany*

Sandip Ghosh

*Department of Condensed Matter Physics and Material Science, Tata Institute of Fundamental Research, Homi Bhabha Road, Mumbai 400005, India*

T. Flissikowski, U. Jahn, and H. T. Grahn

*Paul-Drude-Institut für Festkörperelektronik, Hausvogteiplatz 5-7, 10117 Berlin, Germany*

(Received 25 April 2007; accepted 15 May 2007; published online 7 June 2007)

The authors demonstrate a two-color distributed Bragg reflector (DBR) consisting of 20 periods of alternating  $[1\bar{1}00]$ -oriented (*M*-plane) AlN and GaN layers grown on LiAlO<sub>2</sub> by molecular-beam epitaxy. Due to the birefringent nature of GaN and AlN, the wavelength region of the stop band depends on the polarization state of the incoming light beam (parallel or perpendicular) with respect to the *c* axis of the wurtzite crystal structure. In the wavelength range, where the transmittance for one polarization direction and the reflectance for the orthogonal polarization direction are both high, the DBR can be used as a beam switch or polarization filter. © 2007 American Institute of Physics. [DOI: 10.1063/1.2747189]

The application of multilayer thin films for polarization-sensitive devices has been known for a long time.<sup>1</sup> Polarization-dependent two-color semiconductor mirrors have been demonstrated previously using porous Si structures.<sup>2</sup> Switches and routers are important devices for all-optical computation and communication networks,<sup>3</sup> for which polarizing cube beam splitters<sup>4</sup> are normally used. Here, we present a polarization-dependent beam switch based on group-III-nitride thin films.

Group-III nitrides of the wurtzite crystal structure exhibit linear birefringence, i.e., the refractive index is different for light polarized parallel and perpendicular to the *c* axis.<sup>5-9</sup> In films grown on nonpolar surfaces, where the *c* axis lies in the film plane, this effect can be utilized for beam switching and polarization selection. A distributed Bragg reflector (DBR) with this orientation will exhibit a stop band, whose spectral position and width depends on the linear polarization state of the incident light even at normal incidence. For such a DBR, the transmittance of one polarization direction and the reflectance of the orthogonal polarization direction can be both high in a certain wavelength range. Thus, this DBR can work as a polarization-dependent switch, whereby a linearly polarized light beam under normal incidence is transmitted for one polarization direction (on state) and reflected for the orthogonal polarization direction (off state). A light beam incident at 45° may be transmitted straight through or deflected by 90° depending on its initial polarization state, thereby acting as a polarization-dependent beam router. In addition, an arbitrarily polarized light beam will be split into two components, one parallel and the other perpendicularly polarized to the *c* axis with one component being transmitted and the other one being reflected. In contrast to a DBR with no birefringence, e.g., a *C*-plane GaN/AlN DBR

with identical structural parameters, the efficiency for beam switching and polarization selection can be high over a wide angular range and may exceed 90% at an angle of incidence of 45°.

In this letter, we demonstrate a two-color DBR based on  $[1\bar{1}00]$ -oriented (*M*-plane) GaN and AlN layers grown on  $\gamma$ -LiAlO<sub>2</sub>. The experimental results of transmittance, reflectance, switch gain, and polarization selectivity are compared with simulations based on a transfer-matrix approach.

The prototype DBR was grown on a  $\gamma$ -LiAlO<sub>2</sub>(100) substrate by plasma-assisted molecular-beam epitaxy. The structure consists of 20 periods with nominal thicknesses of 51.6 nm GaN and 43.8 nm AlN on a 313 nm GaN buffer. The entire structure was grown under metal-rich conditions at a temperature of 600 °C for the buffer layer and 750 °C for the DBR.<sup>10,11</sup> For the growth, the substrate was soldered with In on a Si wafer attached to a Mo holder. Prior to the optical measurements, the In was removed by HCl. Since LiAlO<sub>2</sub> is attacked by HCL, this step results in a roughening of the back side of the substrate.<sup>10</sup> For the transmittance and reflectance measurements, the sample was placed at an angle of 45° with respect to the incident light beam and oriented in such a way that the *c* axis was located within the plane of incidence. The probe light was spectrally dispersed by a 0.64 m single monochromator and polarized either parallel or perpendicular to the *c* axis of the wurtzite crystal structure by a Glan-Taylor prism and a  $\lambda/2$  plate. A microscope objective was used to focus the light to a spot of about 50  $\mu$ m diameter on the sample surface. The reflected and transmitted light were detected simultaneously by two Si photodiodes each connected to a lock-in amplifier.

Figure 1 shows a scanning-electron-microscopy (SEM) image of a freestanding piece of the sample. The buffer layer as well as the DBR structure are clearly visible in the magnified image shown in the bottom part of Fig. 1. The structural defects indicated by the arrows are most likely stacking

<sup>a)</sup>Present address: Institut für Angewandte Physik, Universität Karlsruhe (TH), 76128 Karlsruhe, Germany.

<sup>b)</sup>Electronic mail: brandt@pdi-berlin.de

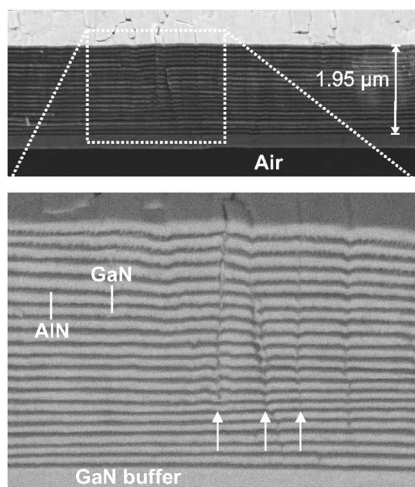


FIG. 1. SEM image of a freestanding  $M$ -plane GaN/AlN distributed Bragg reflector grown on a GaN buffer layer after peeling off from the LiAlO<sub>2</sub> substrate. The arrows in the center of the lower part mark structural defects, which are most likely due to stacking faults.

faults,<sup>12</sup> which disturb the interfaces between the AlN and the GaN layers.

To perform a simulation of the transmittance and reflectance of a birefringent DBR, the  $4 \times 4$  transfer-matrix formalism, as developed by Schubert,<sup>13</sup> is used. The individual layers are assumed to have the nominal thicknesses given above. The coordinate system is chosen such that the  $z$  axis is parallel to the  $c$  axis of the wurtzite crystal structure and the  $y$  axis is parallel to the growth direction.

For this coordinate system, the dielectric tensor is given by

$$\varepsilon = \begin{pmatrix} n_o^2 & 0 & 0 \\ 0 & n_o^2 & 0 \\ 0 & 0 & n_e^2 \end{pmatrix}, \quad (1)$$

where  $n_o$  denotes the ordinary and  $n_e$  the extraordinary refractive index. We have used interpolated experimental values for  $n_o$  and  $n_e$  from Shokhovets *et al.*<sup>14</sup> for our calculations. For a DBR consisting of  $m$  alternating layers of GaN and AlN on a GaN buffer, as shown in Fig. 1, the transfer matrix  $M$  of the whole structure is given by

$$M = L_S^{-1} (T_{\text{GaN}} T_{\text{AlN}})^m T_{\text{GaN}}^{\text{buf}} T_{\text{LAO}} L_F, \quad (2)$$

where  $L_S$  and  $L_F$  are the transfer matrices from air into the DBR and from the substrate into air, and  $T_{\text{AlN}}$ ,  $T_{\text{GaN}}$ ,  $T_{\text{GaN}}^{\text{buf}}$ , and  $T_{\text{LAO}}$  are the transfer matrices for the AlN and GaN layers, the GaN buffer layer, and the substrate, respectively. The exact formulas and method to calculate the transfer matrices, the transmittances  $T_{\parallel}$  and  $T_{\perp}$ , and the reflectances  $R_{\parallel}$  and  $R_{\perp}$  for beams polarized parallel and perpendicular to the  $c$  axis, respectively, are described in Ref. 13. The calculated results were convoluted with a Gaussian function with a standard deviation of 0.15 nm to account for the spectral resolution of the measurement setup.

The results of the simulations for the reflectance and transmittance are shown in Figs. 2(a) and 2(c), respectively. Two distinct stop bands are clearly visible, one for polarization parallel to the  $c$  axis centered at 425 nm and the other for perpendicular polarization centered at 420 nm. The magnitude of the shift between the stop bands is determined by the difference of  $n_o$  and  $n_e$ . In the wavelength region from

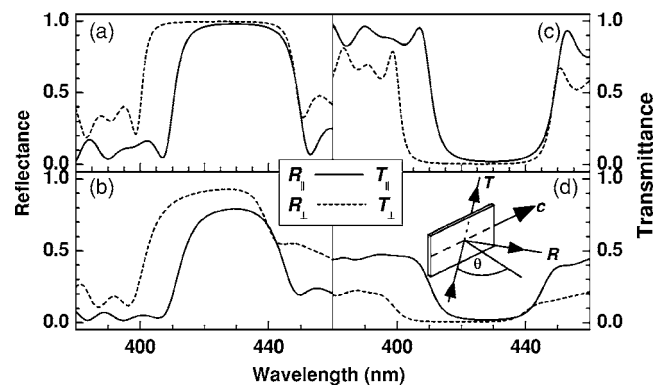


FIG. 2. (a) Simulated and (b) measured reflectance  $R$  vs wavelength for polarizations parallel (solid line) and perpendicular (dashed line) to the  $c$  axis. (c) Simulated and (d) measured transmittance  $T$  vs wavelength for polarizations parallel (solid line) and perpendicular (dashed line) to the  $c$  axis. The shift of the stop band in the reflectance and transmittance curves for different polarizations is clearly visible. The inset in (d) shows the measurement geometry, where  $\theta$  denotes the angle of incidence.

395 to 405 nm, the reflectance  $R_{\perp}$  of light polarized perpendicular to the  $c$  axis in Fig. 2(a) and the transmittance  $T_{\parallel}$  of light polarized parallel to the  $c$  axis in Fig. 2(c) are both high.

For both polarizations, the reflectances and transmittances shown in Figs. 2(b) and 2(d), respectively, were measured simultaneously on the DBR. The inset of Fig. 2(d) displays the measurement configuration with the  $c$  axis located within the plane of incidence. Similar to the simulated results in Fig. 2(a), the reflectance curves in Fig. 2(b) exhibit a stop band, whose central wavelength depends on the state of polarization of the incoming light. For perpendicular polarization the stop band is centered at 425 nm, while for parallel polarization the stop band narrows and spectrally shifts to longer wavelengths centered at 435 nm. Note that a rotation of the DBR by  $90^\circ$  so that the  $c$  axis is perpendicular to the plane of incidence results in the opposite behavior: the stop band for parallel polarization spectrally shifts to shorter wavelengths. The measured reflectance reaches values of only 90% due to the presence of interface and surface roughness. More importantly, however, is the rather low value of the transmittance, which is caused by randomly scattered light at the roughened back side of the substrate.

If the DBR is placed at  $45^\circ$  with respect to the incident beam, light polarized parallel to the  $c$  axis will be transmitted, while light polarized perpendicular to the  $c$  axis will be reflected. A switch gain can be defined as the product of  $T_{\parallel}$  and  $R_{\perp}$ , yielding a figure of merit for the beam switchability of the DBR. The wavelength dependence of the simulated

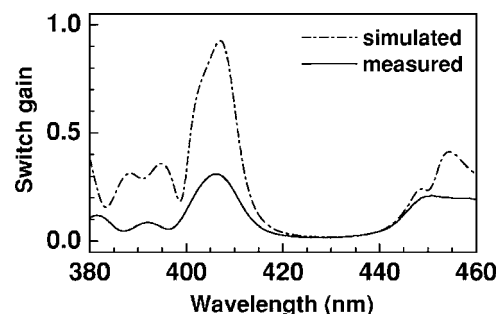


FIG. 3. Measured (solid line) and simulated (dash-dotted line) switch gain as defined by the product of  $T_{\parallel}$  and  $R_{\perp}$  vs wavelength.

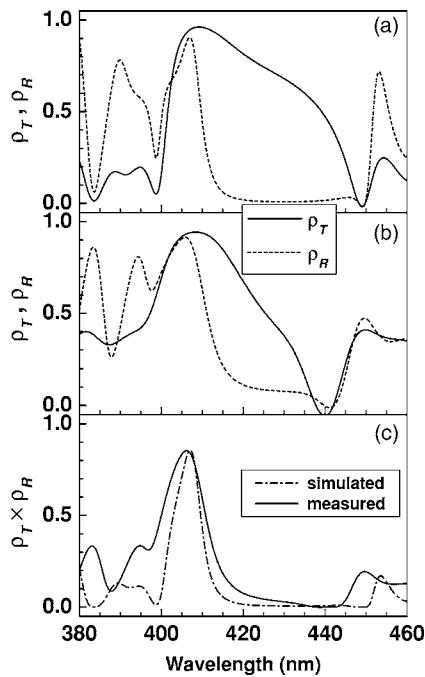


FIG. 4. (a) Simulated and (b) from the measured values calculated degree of polarization for the transmittance ( $\rho_T$ , solid line) and reflectance ( $\rho_R$ , dashed line) vs wavelength. (c) Measured (solid line) and simulated (dash-dotted line) polarization selectivity as defined by the product of  $\rho_T$  and  $\rho_R$  vs wavelength.

switch gain is shown in Fig. 3 by the dashed-dotted line. The maximum switch gain that can be theoretically achieved is about 92%. In contrast, the measured switch gain of the DBR shown in Fig. 3 by the solid line is only about 30%, much lower than the theoretically possible value. This discrepancy is caused by the strong reduction of the transmittance due to stray light losses at the rough back side of the substrate.

The DBR may also be used as a polarization filter, i.e., an arbitrarily polarized light beam will be split into two components: one parallel (transmitted) and the other one perpendicularly polarized (reflected) to the  $c$  axis. Figure 4(a) displays the simulated degrees of polarization  $\rho_T$  and  $\rho_R$  for the transmitted and reflected beams, respectively,

$$\rho_T = \frac{T_{\parallel} - T_{\perp}}{T_{\parallel} + T_{\perp}},$$

$$\rho_R = \frac{R_{\perp} - R_{\parallel}}{R_{\parallel} + R_{\perp}}. \quad (3)$$

Experimentally, one observes very similar curves, as shown in Fig. 4(b). The previously discussed effects that reduce the

switch gain have much less influence on the degree of polarization because of the normalization. The experimental results are in good agreement with the simulations, indicating once more that the DBR operates as expected.

The operation regime for polarization selection falls theoretically into the wavelength range, where both the reflected and the transmitted beam exhibit a large degree of polarization. The simulated polarization selectivity defined as the product of  $\rho_T$  and  $\rho_R$  is shown as a function of wavelength in Fig. 4(c) by the dashed-dotted line. The highest selectivity of 85% is achieved around 410 nm. The measured polarization selectivity shown in Fig. 4(c) by the solid line also peaks at about the same wavelength.

We have fabricated a two-color distributed Bragg reflector consisting of 20 periods of  $M$ -plane AlN and GaN layers grown on LiAlO<sub>2</sub>. Due to the birefringent character of the wurtzite crystal structure, the spectral position of the stop band depends on the state of polarization, i.e., parallel or perpendicular to the  $c$  axis. We have demonstrated that this birefringent DBR offers two main functionalities, polarization-dependent beam switching and polarization selection. When the DBR is rotated around the  $y$  axis by 45°, a third functionality, namely, polarization rotation, is available. In this mode, the polarization state of the incoming light is rotated by 90° in transmission or reflection due to a cross coupling of the two polarization states parallel and perpendicular to the  $c$  axis.

<sup>1</sup>P. B. Clapham, M. J. Downs, and R. J. King, *Appl. Opt.* **8**, 1965 (1969).

<sup>2</sup>J. Diener, N. Künzner, D. Kovalev, E. Gross, V. V. Timoshenko, G. Polisski, and F. Koch, *Appl. Phys. Lett.* **78**, 3887 (2001).

<sup>3</sup>C. Vazquez, J. M. S. Pena, S. E. Vargas, A. L. Aranda, and I. Perez, *IEEE Sens. J.* **3**, 513 (2003).

<sup>4</sup>J. Mouchart, J. Begel, and E. Duda, *Appl. Opt.* **28**, 2847 (1989).

<sup>5</sup>A. S. Barker and M. Illegems, *Phys. Rev. B* **7**, 743 (1973).

<sup>6</sup>H. Amano, N. Watanabe, N. Koide, and I. Akasaki, *Jpn. J. Appl. Phys., Part 2* **32**, L1000 (1993).

<sup>7</sup>T. Kawashima, H. Yoshikawa, S. Adachi, S. Fuke, and K. Ohtsuka, *J. Appl. Phys.* **82**, 3528 (1997).

<sup>8</sup>U. Tisch, B. Meyler, O. Katz, E. Finkman, and J. Salzman, *J. Appl. Phys.* **89**, 2676 (2001).

<sup>9</sup>S. Ghosh, P. Waltereit, O. Brandt, H. T. Grahn, and K. H. Ploog, *Appl. Phys. Lett.* **80**, 413 (2002).

<sup>10</sup>Y. J. Sun, O. Brandt, and K. H. Ploog, *J. Vac. Sci. Technol. B* **21**, 1350 (2003).

<sup>11</sup>O. Brandt, Y. J. Sun, L. Däweritz, and K. H. Ploog, *Phys. Rev. B* **69**, 165326 (2004).

<sup>12</sup>Y. J. Sun, O. Brandt, U. Jahn, T. Y. Liu, A. Trampert, S. Cronenberg, S. Dhar, and K. H. Ploog, *J. Appl. Phys.* **92**, 5714 (2002).

<sup>13</sup>M. Schubert, *Phys. Rev. B* **53**, 4265 (1996).

<sup>14</sup>S. Shokhovets, R. Goldhahn, G. Gobsch, S. Piekh, R. Lantier, A. Rizzi, V. Lebedev, and W. Richter, *J. Appl. Phys.* **94**, 307 (2003).